Metabolic Insertion of Nanostructured TiO_2 into the Patterned Biosilica of the Diatom *Pinnularia* sp. by a Two-Stage Bioreactor Cultivation Process

Clayton Jeffryes,[†] Timothy Gutu,[‡] Jun Jiao,[‡] and Gregory L. Rorrer[†,*]

[†]Department of Chemical Engineering, Oregon State University, Corvallis, Oregon 97331, and [‡]Department of Physics, Portland State University, Portland, Oregon 97207

ABSTRACT Diatoms are single-celled algae that make silica shells or frustules with intricate nanoscale features imbedded within periodic two-dimensional pore arrays. A two-stage photobioreactor cultivation process was used to metabolically insert titanium into the patterned biosilica of the diatom *Pinnularia* sp. In Stage I, diatom cells were grown up on dissolved silicon until silicon starvation was achieved. In Stage II, soluble titanium and silicon were continuously fed to the silicon-starved cell suspension ($\sim 4 \times 10^5$ cells/mL) for 10 h. The feeding rate of titanium (0.85−7.3 μmol Ti L^{-1} h^{-1}) was designed to circumvent the precipitation of titanate in the liquid medium, and feeding rate of silicon (48 μmol Si L^{-1} h^{-1}) was designed to sustain one cell division. The addition of titanium to the culture had no detrimental effects on cell growth and preserved the frustule morphology. Cofeeding of Ti and Si was required for complete intracellular uptake of Ti. The maximum bulk composition of titanium in the frustule biosilica was 2.3 g of Ti/100 g of SiO_2. Intact biosilica frustules were isolated by treatment of diatom cells with SDS/EDTA and then analyzed by TEM and STEM-EDS. Titanium was preferentially deposited as a nanophase lining the base of each frustule pore, with estimated local TiO_2 content of nearly 80 wt %. Thermal annealing in air at 720 °C converted the biogenic titanate to anatase TiO_2 with an average crystal size of 32 nm. This is the first reported study of using a living organism to controllably fabricate semiconductor TiO_2 nanostructures by a bottom-up self-assembly process.

KEYWORDS: cell culture · diatoms · TiO_2 · nanophase

Nanostructured titanium dioxide (TiO_2) semiconductor materials have unique optoelectronic properties that enable a variety of applications, particularly for photocatalysts and solar cells.[1] Control of the spatial organization of nanoscale TiO_2 within a periodic structure offers additional enhancements for light trapping in these applications.[2] There is enormous interest in bioinspired approaches for synthesis of semiconductor and metal oxide nanomaterials, as they offer the opportunity for self-assembly into hierarchical structures.[3] In particular, cell culture systems have been identified as a platform for the biosynthesis of photonic nanostructures.[4] Although biomineralization of TiO_2 is rare in Nature,[5] biosilica (amorphous SiO_2) is synthesized from soluble silicon into complex structures by a variety of aquatic organisms, as exemplified by the diatoms.[6] Diatoms are single-celled algae which make silica shells called frustules that are intricately patterned at both the nano- and microscale. The periodic pore structures of diatoms possess photonic crystal properties.[7]

Traditionally, the bioinspired synthesis of titanate materials has focused on the biomolecule-mediated precipitation of soluble titanium precursors using peptide sequences derived from the silaffin class of diatom proteins,[8−10] phage-displayed peptides,[11] recombinant silicatein proteins derived from sponge spicules,[12−14] naturally occurring polyamines,[15] lysozymes,[16] or proteins secreted from bacterial or fungal cell surfaces.[17,18] Alternatively, diatom frustules have served as a template for synthesis of nano/microstructured titanate materials using a variety of chemical processes, including gas−solid reaction of biosilica with TiF_4 vapor,[19,20] atomic layer deposition of $TiCl_4/H_2O$ vapor,[21] or solution phase coating of TiO_2 nanoparticles.[22] To date, biomolecule-mediated precipitation processes have not yet organized TiO_2 into hierarchical structures, and diatom-based templating methods have not been designed to be readily scalable.

In this study, we use the living diatom itself to metabolically insert nanostructured TiO_2 into the periodic structure of its frustule biosilica. The intracellular biofabrication process is guided by a two-stage photobioreactor cultivation process that controls the delivery of titanium and silicon to the diatom cells. This bioprocess engineering approach is scalable, replicates identical nanostructures on a massively parallel scale, occurs at ambient temperature and neutral

*Address correspondence to rorrergl@engr.orst.edu.

Received for review July 25, 2008 and accepted September 15, 2008.

Published online October 2, 2008.
10.1021/nn800470x CCC: $40.75

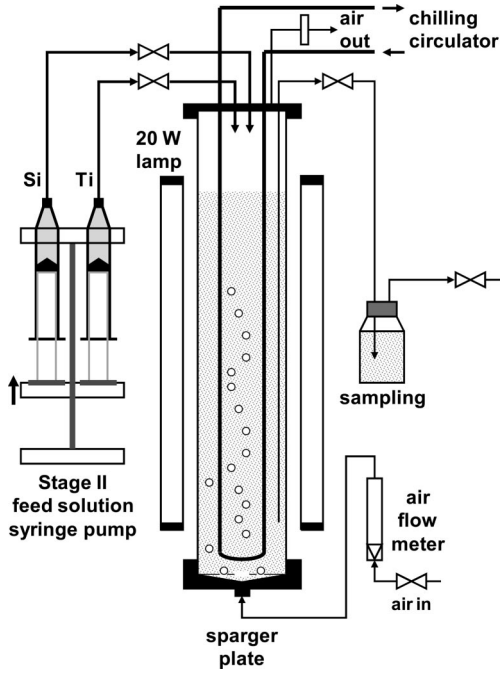

Figure 1. Photobioreactor for cultivation of the diatom *Pinnularia* sp. under controlled delivery of soluble silicon and titanium.

pH, and does not require harsh chemicals or sophisticated equipment. *Pinnularia* sp. was chosen as the model diatom because its frustule possesses periodic order at two scales: a rectangular lattice of 200 nm pores at the submicron scale, and a concentric array of fine features lining the base of each pore at the nanoscale.

Diatoms are known to bioaccumulate trace levels of titanium,[23] where organisms collected from the marine environment can contain 0.01 to 0.13 wt % Ti in silica.[24] However, the controlled cultivation of diatom cells on soluble titanium has not been previously reported. One challenge is the low solubility of $Ti(OH)_4$ in aqueous solution at the cultivation pH. Below, we show how controlled feeding of soluble silicon and titanium to the cells during the bioreactor cultivation process circumvents this solubility limitation and targets the deposition of a TiO_2-rich nanophase into the periodic fine features associated with the pores of the diatom frustule. We also show that thermal annealing converts the biogenic titanate to anatase TiO_2 nanocrystals.

RESULTS AND DISCUSSION

Bioreactor Cultivation for Metabolic Insertion of Titanium into Frustule Biosilica. A two-stage photobioreactor cultivation process was used to grow up *Pinnularia* diatom cells to a desired cell density and then metabolically insert titanium into the frustule biosilica. The photobioreactor presented in Figure 1 consisted of a bubble column bioreactor vessel to mix and aerate the cell suspension, an external light stage, and a syringe pump for controlled delivery of soluble silicon and titanium.

TABLE 1. Cultivation Parameters for Two-Stage Bioreactor Cultivation of *Pinnularia* sp. Cells

process parameter	Stage I	Stage II
initial Si concentration (mM)	0.50	~0
initial Ti concentration (mM)	0.00	0
initial cell number density (10^5 cells mL^{-1})	0.50	*a*
total culture volume (L)	4.2	3.1
Si and Ti delivery rate		
volumetric flowrate (mL feed L^{-1}culture h^{-1})[a]	—	3.3
feed solution Ti concentration (mM)	—	0.5—4.5
feed solution Si concentration (mM)	—	30
Ti delivery rate (μmol Ti L^{-1} culture h^{-1})	—	0.85—7.3
Si delivery rate (μmol Si L^{-1} culture h^{-1})	—	48
time of addition (h)	—	10
total Si added (μmol Si/L culture)	—	480
total Ti added (μmol Ti/L culture)	—	8.5—73
input mol Si/mol Ti	—	6.5—56
cultivation pH	8.4	8.6
temperature (°C)	22	22
incident light intensity (μE m^{-2} s^{-1})	149	149
photoperiod (h light:h dark in 24 h)	14:10	14:10
aeration rate (L air L^{-1} culture min^{-1})	0.61	0.82
CO_2 partial pressure (ppm)	~350	~350
cultivation time (h)	120	72

[a] 5.0 mL h^{-1} for each feed solution.

In Stage I of the cultivation process, the cell suspension was grown up on a given initial concentration of dissolved silicon (0.50 mM) until all the silicon was consumed and the final cell density was achieved. In Stage II of cultivation, concentrated feed solutions of 30 mM sodium metasilicate and soluble titanate (0.5—4.5 mM) were co-delivered to the culture suspension by a syringe pump over a period of 10 h during the light phase of the first photoperiod, as detailed in Table 1.

Cell number density and dissolved silicon concentration *versus* time for Stages I and II of a representative bioreactor cultivation experiment are presented in Figure 2a. Images of living cells and frustule biosilica at the end of Stage I, just before addition of titanium to the cultivation medium, are presented in Figure 2b,c. Silicon was a required substrate for diatom cell division. At the end of Stage I cultivation, the diatom cells were in the silicon-starved state, as evidenced by complete consumption of dissolved silicon from the medium and constant cell number density for at least one 24 h photoperiod. The cumulative amount of Si delivery was designed to support one cell division within the first photoperiod of Stage II. The Si delivery rate was fixed, whereas the Ti delivery rate was varied by changing the Ti concentration in the feed solution. However, within a given cultivation experiment, the ratio of Ti/Si delivered to the cell suspension was constant. When the soluble silicon feed solution was added to the culture medium, it speciated to $Si(OH)_4$ at the cultivation pH of 8.5, which is the form of Si required for transport into the diatom cell.[25]

Representative Si and Ti concentration profiles in the bioreactor cultivation medium during the first 48 h

TABLE 2. Growth Parameters from the Two-Stage Bioreactor Cultivation of *Pinnularia* sp. Cells

Ti addition (μmol/L)	Stage	specific growth rate μ (h^{-1})	cell number yield [a] $Y_{Xn/Si}$ (10^8 cells/mmol Si)	cell number density $X_{N,f}$ (10^5 cells mL^{-1})
(control)	I	0.032 ± 0.003	10.8 ± 1.1	5.9 ± 0.2
0.0	II	0.039 ± 0.008	12.0 ± 1.2	12.1 ± 0.9
	I	0.031 ± 0.003	8.9 ± 1.9	3.7 ± 0.4
8.5	II	0.024 ± 0.005	13.5 ± 1.7	9.9 ± 1.1
	I	0.035 ± 0.001	9.5 ± 2.2	4.7 ± 0.6
14	II	0.043 ± 0.008	12.3 ± 1.4	12.1 ± 1.0
	I	0.043 ± 0.004	8.2 ± 1.7	4.8 ± 0.4
22	II	0.032 ± 0.006	11.3 ± 1.3	10.8 ± 1.1
	I	0.018 ± 0.003	7.4 ± 1.6	4.3 ± 0.1
49	II	0.029 ± 0.006	12.2 ± 0.7	9.6 ± 0.4
	I	0.021 ± 0.002	9.4 ± 1.6	4.1 ± 0.4
73	II	0.032 ± 0.003	12.9 ± 2.8	9.6 ± 2.0

[a] The Stage II average cell number to dry cell mass ratio is $3.05 \times 10^9 \pm 4.14 \times 10^8$ cells/g DW.

of Stage II cultivation are presented in Figure 3. In Figure 3a, if no cells were present, then Si and Ti were not consumed, and the measured Si and Ti concentration *versus* time profile matched the predicted profile delivered by the syringe pump. The titanium concentration represented both the soluble and insoluble titanium in the liquid medium. Figure 3b shows that the diatom cells consumed most of the Si fed to the culture over the 10 h delivery period, providing enough silicon for one cell doubling (Figure 2a). The dissolved silicon concentration in the medium was near zero at all times, which indicated that the cells were maintained in the silicon-starved state during Stage II. Likewise, Figure 3c

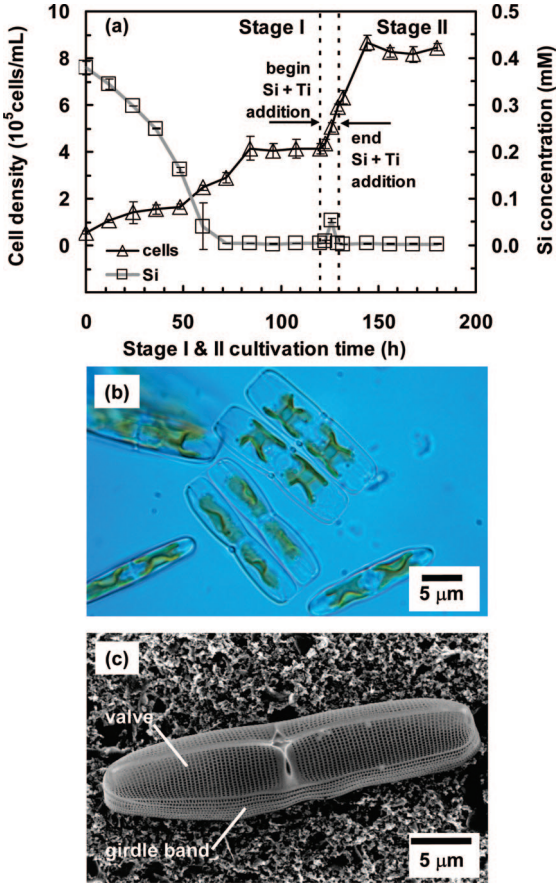

Figure 2. Bioreactor cultivation of *Pinnularia* sp. cells. (a) Cell number density and dissolved silicon concentration *versus* time for Stages I and II of bioreactor cultivation, with Stage II cumulative Ti and Si addition of 73 and 480 μmol/L, respectively; (b) light micrograph of living diatom cells at the end of Stage I, just before addition of titanium to the cultivation medium; (c) SEM of frustule biosilica isolated by SDS/EDTA treatment of diatom cells at the end of Stage I, just before addition of titanium to the cultivation medium.

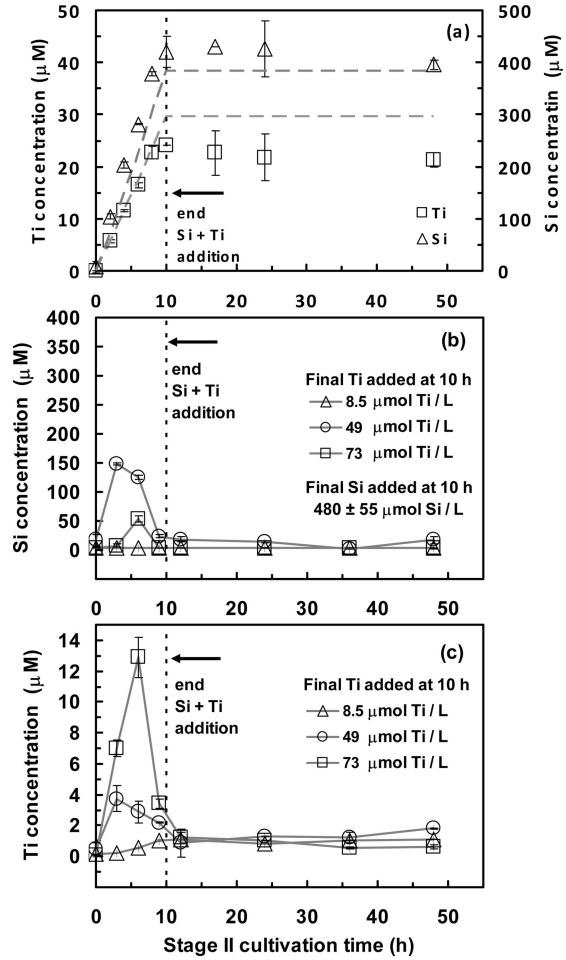

Figure 3. Concentration profiles for Si and Ti in liquid medium during Stage II of cultivation. (a) No-cell control experiment, cumulative addition of 0.37 mM Si and 29 μM Ti; (b) Si concentration in culture *versus* cumulative Ti addition; (c) Ti concentration in culture *versus* cumulative Ti addition.

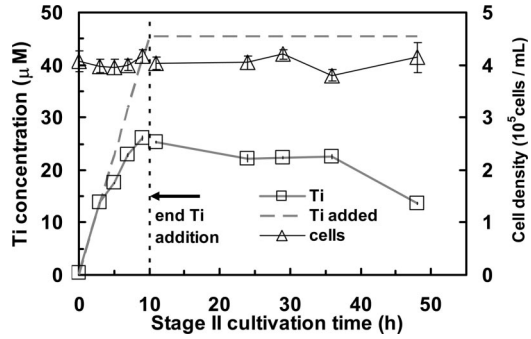

Figure 4. Stage II of control experiment where Ti but no Si was added. Cumulative Ti addition was 46 μM.

shows that the diatom cells also consumed all of the Ti added to the culture suspension at all three cumulative amounts of Ti delivery. At the onset of Stage II, the rate of $Ti(OH)_4$ addition at the highest Ti loading (73 μmol/L) outpaced the rate of intracellular Ti uptake, where the soluble titanium concentration in the liquid phase of the cell culture medium increased to 13 μM before returning to zero.

The Ti concentration in the culture medium generally stayed below the $Ti(OH)_4$ solubility limit. When the soluble titanium feed solution was added to the liquid culture medium, the titanium diluted out and hydrolyzed to $Ti(OH)_4$ at the nominal bioreactor cultivation pH of 8.5. The solubility limit of $Ti(OH)_4$ in 100 mM NaCl at 22 °C is between 3 and 8 μM, and $Ti(OH)_4$ is the dominant soluble species at pH >6.[26,27] Consequently, if titanium was added to the culture suspension all at once, then the concentration of titanium in the liquid medium would have exceeded the reported solubility of $Ti(OH)_4$ by an order of magnitude. Therefore, titanium was delivered at a rate that prevented its potential for precipitation in the culture suspension, as the balance between titanium delivery and uptake by the diatom cells kept the titanium concentration in the culture liquid below its solubility limit. If titanium but no silicon was fed to the diatom cell suspension in Stage II of cultivation, the uptake of titanium was not complete, as shown in Figure 4. The diatom cells did not divide, and the Ti concentration in the liquid medium stayed well above the solubility limit.

The culture growth parameters obtained from the two-stage bioreactor cultivation experiments, including specific growth rate (μ), final cell density ($X_{N,f}$), and cell number yield coefficient based on silicon consumption ($Y_{Xn/Si}$), are summarized in Table 2. The cumulative amount of titanium delivery had no statistically significant effect on either the specific growth rate ($p = 0.60 > \alpha = 0.05$) or the cell number yield coefficient ($p = 0.75 > \alpha = 0.05$). There was no change in specific growth rate between Stages I and II ($p = 0.51 > \alpha = 0.05$). The increase in cell number yield coefficient was statistically significant between Stages I and II ($p = 0.0017 < \alpha = 0.05$), which indicated that the Si content per cell decreased.

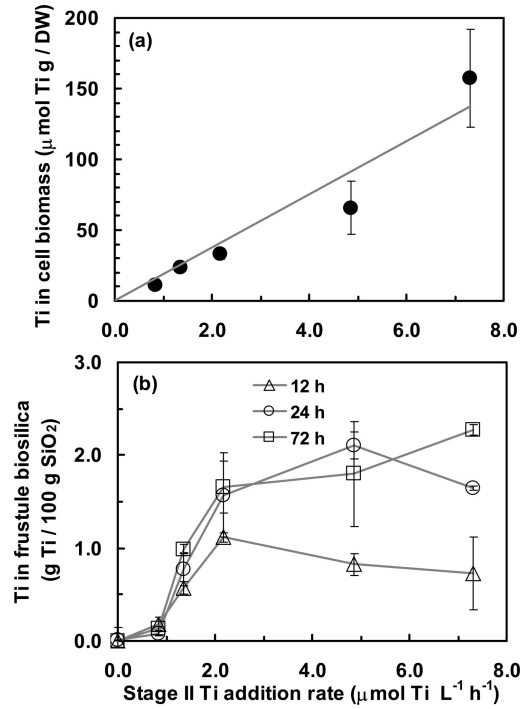

Figure 5. Uptake of titanium by the *Pinnularia* sp. cell suspension as function of Ti addition rate to Stage II of cultivation. (a) Intracellular Ti; (b) Ti retained within frustule biosilica at cultivation times of 12, 24, and 74 h. The total time of Ti and Si addition was 10 h. The cumulative Si addition amount averaged 480 μM over all experiments.

The incorporation of titanium into the diatom cells as a function of the Stage II titanium delivery rate is presented in Figure 5. After 24 h, the intracellular titanium concentration was complete. Figure 5a shows the measured intracellular uptake of titanium into the cell mass, averaged from 24 to 72 h, was linearly proportional to titanium delivery rate. The diatom cells were treated with sodium dodecyl sulfate (SDS) in EDTA to remove organic materials and isolate the intact frustule biosilica. The parent valve and the new daughter valve formed after cell division often remained attached to one another (Figure 2c). The average solids recovery after SDS/EDTA treatment and drying at 80 °C was 0.32 ± 0.07 g solid/g dry biomass weight (DW). Figure 5b shows that the amount of Ti incorporated into the frustule biosilica reached a saturation value, nominally at 2.0 g of Ti/100 g of SiO_2. Furthermore, the final titanium incorporation into the biosilica was not achieved until after 24 h in Stage II, indicating that an intracellular pool of titanium was still being incorporated into the diatom biosilica after titanium delivery to the culture suspension was complete. For the control cultivation experiment where titanium but no silicon was added to Stage II of the cultivation, the intracellular Ti content after 48 h was 95 ± 6 μmol T/g DW.

The concentration of titanium in dried diatom cells, cells treated with SDS/EDTA, and cells treated with aqueous (30 wt %) hydrogen peroxide (H_2O_2) is compared in Table 3. The presence of titanium in the frus-

tule biosilica after treatment of the diatom cells by either SDS/EDTA or H_2O_2 treatment verified that the titanium was imbedded within the frustule silica and not adsorbed onto the frustule surface. The Ti concentration in the H_2O_2-treated frustule biosilica was lower than that in the SDS/EDTA-treated diatom biosilica because titanate imbedded in biosilica close to the frustule surface may have been etched out by aqueous H_2O_2. Consequently, the SDS/EDTA treatment method was used to isolate frustules for the electron microscopy. A material balance on the washings from both treatment methods verified that only about 40−50% of the titanium taken up by the living cells was ultimately incorporated into the frustule biosilica. Control experiments further verified that titanium released by either treatment method did not re-adsorb onto the frustule biosilica. Therefore, the titanium recovered from cell washing and SDS/EDTA treatments was assumed to be weakly bound intracellular titanium.

Titanium-Rich Nanophase within Diatom Biosilica. The nanoscale titanium distribution in the diatom biosilica was characterized by electron microscopy. The diatom cells selected for nanoimaging and analysis were obtained from the bioreactor cultivation experiment conducted at 73 μmol/L cumulative Ti addition to Stage II. Cells harvested after 72 h into Stage II were treated with SDS/EDTA to remove organic materials and isolate the intact frustule biosilica. The bulk titanium concentration in the biosilica was 2.3 ± 0.1 g of Ti/100 g of SiO_2. Ten randomly selected frustules were analyzed by transmission electron microscopy (TEM) and scanning transmission electron microscopy/X-ray dispersive analysis (STEM-EDS). Representative analyses were reported.

STEM-EDS analyses of a representative *Pinnularia* sp. frustule containing titanium are presented in Figure 6. The spot scan in Figure 6b shows that Si, Ti, and O were the only elements present, as Cu was from the copper TEM grid. The representative line scans shown Figure 6c,d spanned the whole width (line scan 1) and length (line scan 2) of the frustule. The line scans included both solid regions and pore regions. The peaks of titanium concentration always coincided with the base of the 200 nm frustule pores. Ti was found everywhere in the frustule biosilica, including the valve (top face) and girdle band (side wall) regions, but it was not uniformly distributed. In particular, line scan 1 showed that high concentration pockets of titanium were associated with both the valve (top face) and girdle band (side wall) of the frustule. Line scan 2 also showed periodic regions of high titanium concentration. The line scan presented in Figure 6e,f was aligned between two valve halves that were still partially adjoined after SDS treatment. Here, it is shown that the titanium was preferentially deposited into the new daughter valve of frustule. All of the line scans shown in Figure 6 were obtained at a scanning interval ranging from 178 to 246

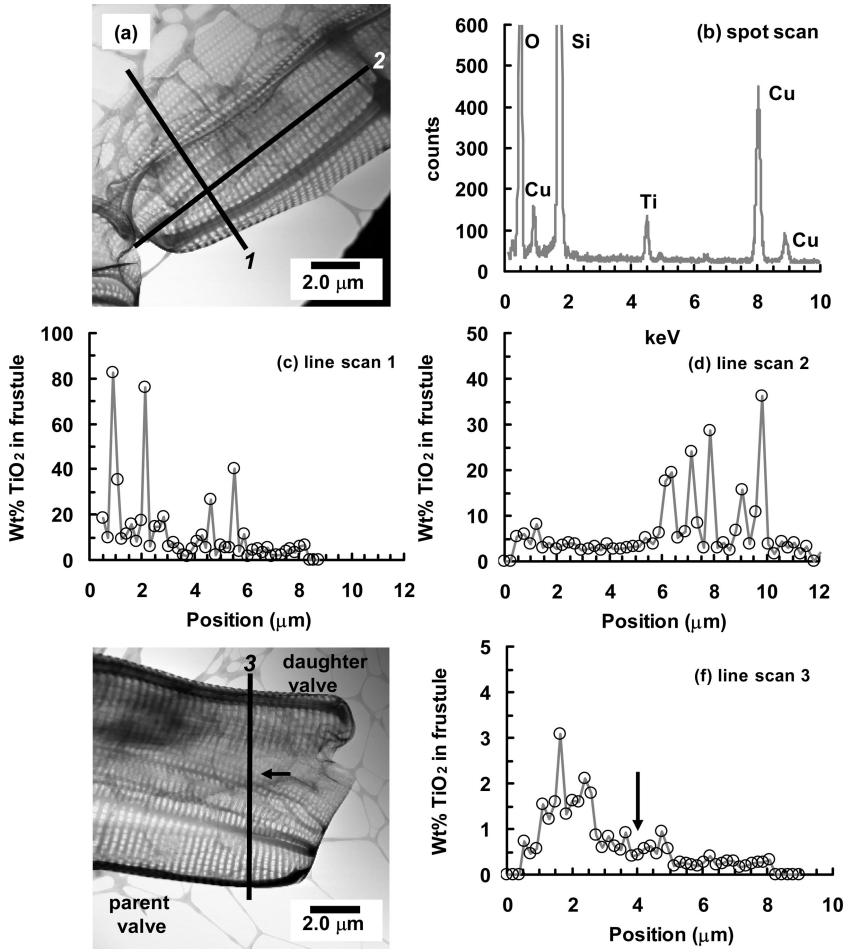

Figure 6. STEM-EDS analysis of frustule biosilica containing metabolically inserted titanium. (a) STEM image with two line scan traces; (b) representative spot scan; (c) TiO_2 profile along width of frustule, spanning valve and girdle band (line scan 1); (d) TiO_2 profile down length of frustule valve (line scan 2); (e,f) STEM image with line scan across the transverse axis of two adjoined frustules, starting from the daughter valve and then crossing over to the parent valve (line scan 3).

TABLE 3. Comparison of Ti Recovery after SDS/EDTA and H_2O_2 Treatment of Diatom Cells Containing Metabolically Inserted Titanium

sample	bulk Ti concentration (g of Ti/100 g of SiO_2)	% intracellular Ti removed by treatment method
dry cell biomass	3.8 ± 0.8	
SDS/EDTA-treated cells	2.3 ± 0.1	41 ± 8
H_2O_2-treated cells	1.9 ± 0.1	49 ± 10

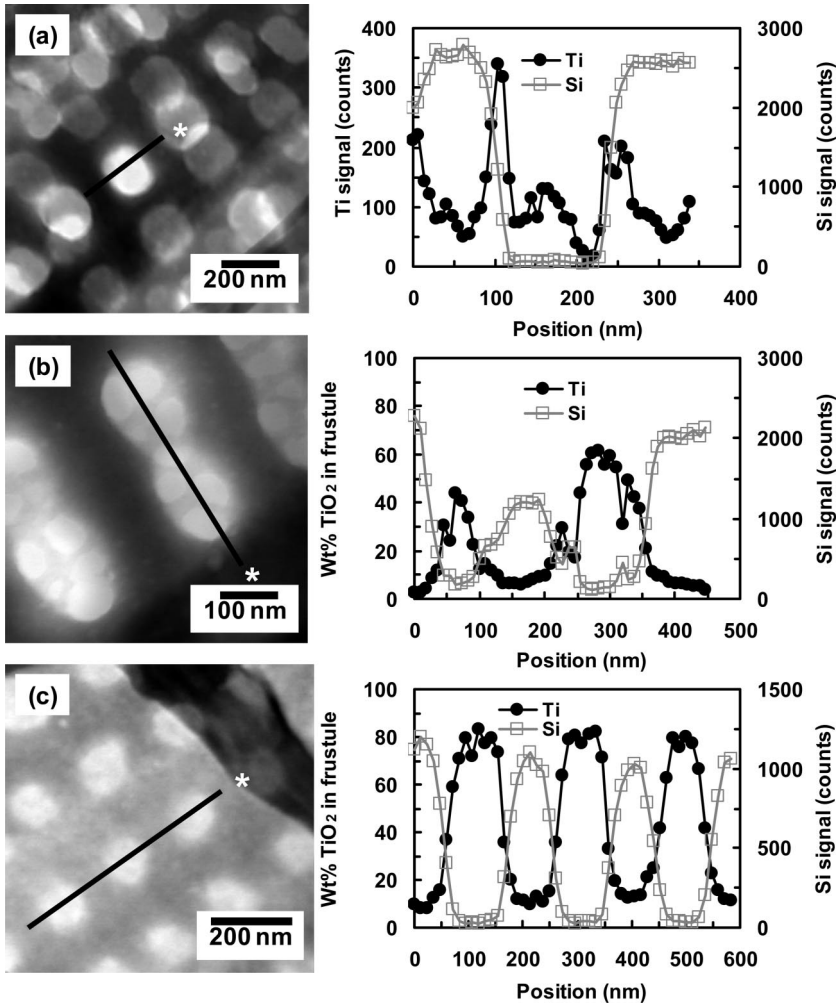

Figure 7. STEM-EDS elemental line scan of Ti and Si across frustule pores, revealing Ti-rich nanophase lining base of pore. (a) Single pore; (b) two fused pores; (c) three pores.

nm, which was not precise enough to guarantee that the beam always hit the base of the 200 nm pore.

STEM-EDS line scans for titanium and silicon across three representative pore structures are presented in Figure 7. The scanning interval was set to 7−12 nm so that the nanoscale features could be more readily profiled. In the diatom *Pinnularia* sp., the base of each 200 nm frustule pore is lined with a thin layer of biosilica which contains 4−6 pores nominally 50 nm in diameter. In STEM mode, these fine features were difficult to see. However, the elemental line scans clearly showed that the base of the frustule pore was highly enriched in titanium. In Figure 7a, a comparison of the Ti and Si line scan data revealed that the highest Ti signal counts were concentrated near the frustule pore wall. However, the Si signal count was also high in this region, so the Ti concentration in the biosilica was still relatively low. In contrast, for the metal oxide materials lining the base of the frustule pore, the Ti signal count was high, but the Si signal count was low, and so the Ti concentration was high. The nanoscale thickness of the frustule was not measured due to its complicated topology. However, the combined Si and Ti signal count was roughly indicative of the relative thickness of the frustule.

Quantitative line scans for TiO_2 along two other representative pore structures are presented in Figure 7b,c. The TiO_2 was enriched from 40 to 80% at the base of the pore. However, it must be stressed that the quantification was only approximate since EDS measurement is dependent upon X-ray beam penetration and scattering into the sample[28] as well as the surface roughness.[29] The bulk TiO_2 concentration in the frustule (3.7 wt % TiO_2 based on 2.3 g of Ti/100 g of SiO_2) was still much lower than the local TiO_2 concentration because the volume of solid associated with these fine features was small relative to the overall volume of the frustule solid. Furthermore, the bulk TiO_2 content was diluted from the biosilica carried over from Stage I of the cultivation.

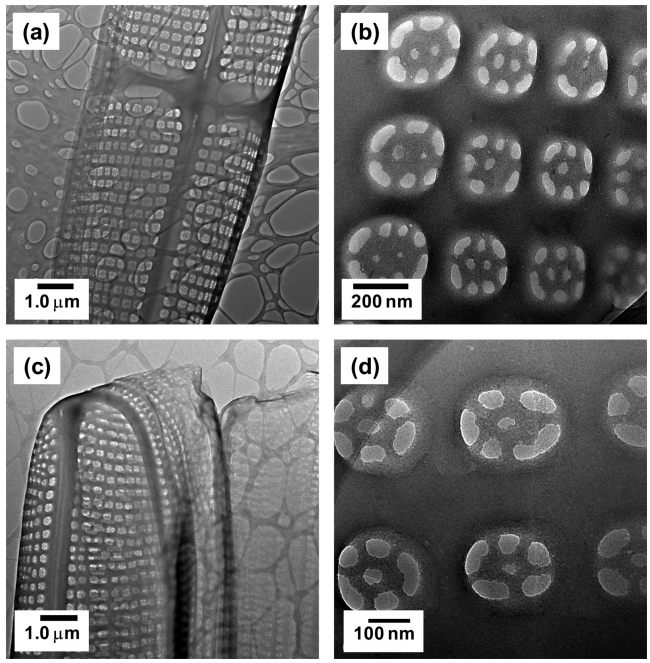

Figure 8. TEM images of frustule biosilica. (a,b) Frustule from control cultivation experiment; (c,d) frustule containing titanium analyzed by STEM-EDS in Figure 7.

Figure 8 compares TEM images of fine structure for the *Pinnularia* frustule with and without titanium metabolically inserted into the biosilica. Figure 8a,b shows frustules from the control cultivation experiment with no added titanium, whereas Figure 8c,d shows frustules from the cultivation experiment where the cumulative addition of titanium to Stage II was 73 μmol/L (2.3 g of Ti/100 g of SiO_2). The same frustule shown in Figure 8d was analyzed earlier by STEM-EDS (Figure 7). In TEM

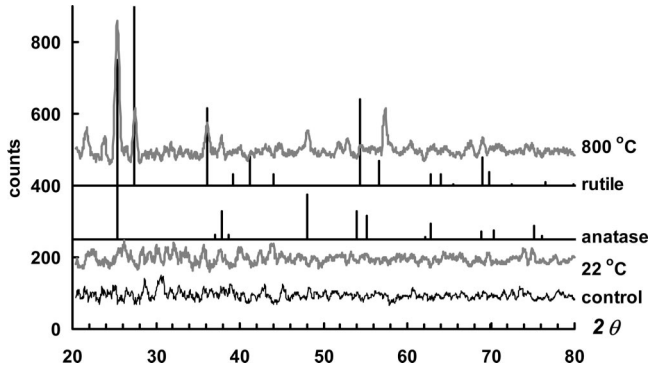

Figure 9. Powder X-ray diffraction spectra of frustule biosilica containing 2.3 g of Ti/100 g of SiO_2 in the as-deposited state (22 °C) and after thermal annealing in air (800 °C). For comparison, XRD spectra of the following are also provided: diatom biosilica thermally annealed at 800 °C containing no titanium (control), an anatase TiO_2 standard (JCPDS 86-1156), and a rutile TiO_2 standard (JCPDS 86-0148).

mode, the fine features at the base of the frustule pores were clearly visible. The incorporation of titanium into the frustule biosilica did not alter the overall pore structure of the frustules or its fine features imbedded at the base of each pore.

In summary, the metabolic insertion of TiO_2 into the diatom biosilica targeted the fine nanostructure lining the base of each frustule pore and did not alter the overall microstructure of the diatom. In contrast, our earlier studies[30−32] showed that metabolic insertion of germanium into diatom biosilica altered the frustule pore structure by reducing the pore diameter, removing the fine features, and fusing the pore arrays into nanoslit arrays. Therefore, there were marked differences in the mechanisms of GeO_2 *versus* TiO_2 incorporation into the diatom biosilica. However, it was beyond the scope of this work to characterize the molecular processes underlying these differences.

Annealing of Ti-Rich Nanophases in Frustule Biosilica to Nanocrystalline TiO_2. Thermal annealing of diatom biosilica containing titanium converted the biogenic titanates to crystalline TiO_2. The sample profiled in Figures 6−8 was annealed at 720, 800, and 950 °C. The powder X-ray diffraction (XRD) spectra presented in Figure 9 show that the as-deposited diatom biosilica containing 2.3 ± 0.1 g of Ti/100 g of SiO_2 was amorphous. However, at an annealing temperature of 800 °C, a mixture of anatase and rutile phases of crystalline TiO_2 were formed. Thermal annealing of the no-titanium diatom biosilica control sample at 800 °C verified that the diatom biosilica itself remained amorphous. Increasing the annealing temperature 720 to 950 °C changed TiO_2 from the anatase from to the rutile form (Figure 10). The average nanocrystal size estimated by the Scherer equation for both the anatase and rutile forms of TiO_2 was about 32 nm. The possibility Ti−O−Si bond formation was not considered by this study.

The TiO_2-rich nanophases that were imbedded within the frustule biosilica after metabolic insertion of titanium were amorphous. Previous investigators found that the peptide- or protein-mediated precipitation of soluble titanium precursors to TiO_2 or TiP_2O_7 was also amorphous at room temperature but could be crystallized by thermal annealing.[9,10,12] In a few studies, biomimetic approaches have produced crystalline forms of TiO_2 without thermal annealing. Kröger *et al.*[8] observed that TiBALDH precipitation by the recombinant silaffin protein rSilC produced rutile TiO_2, whereas Dickerson *et al.*[11] observed that 12-mer phase display peptides produced a mixture of amorphous, anatase, and monoclinic (β) forms of TiO_2. Bansal *et al.*[17] precipitated K_2TiF_6 with proteins secreted from the fungus *Fusarium oxysporum* to the brookite form of TiO_2 at ambient temperature. No biomimetic studies to date have fabricated nanoscale TiO_2 into hierarchical structures as demonstrated by this study.

Processes Underlying TiO_2 Nanophase Formation within Frustule Biosilica. The distribution of TiO_2 within the periodic structure of the *Pinnularia* sp. frustule is schematically envisioned in Figure 11. We speculate that rate processes of SiO_2 and TiO_2 formation within the silica deposition vesicle of the dividing diatom cell may have led to the preferential deposition of TiO_2 at the thin layer of biosilica lining the base of the frustule pore, as proposed below.

The biofabrication of the biosilica frustule within the silica deposition vesicle (SDV) has been described for pennate diatoms in general[33,34] and *Pinnularia* species in particular.[35] Within this framework, a phase separation model for biosilicification within the SDV has been proposed[36,37] where formation in the pore spaces (areolae) occurs after silicification of the rib structures (costae). Hildebrand *et al.*[38] has verified these steps of frustule formation in the centric diatom *Thalassiosira* by SEM, TEM, and atomic force microscopy (AFM) measurements.

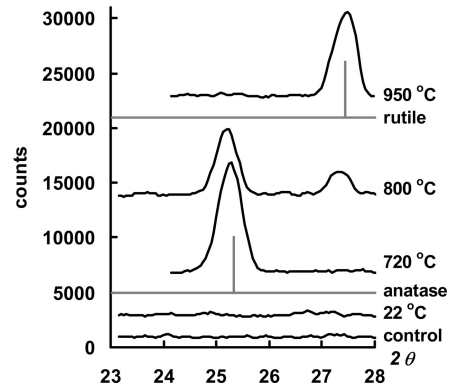

Figure 10. Effect of thermal annealing temperature on the XRD spectra of frustule biosilica containing 2.3 g of Ti/100 g of SiO_2. Biogenic TiO_2 was converted from amorphous to anatase TiO_2 and to rutile TiO_2. The "control" refers to frustule biosilica containing no titanium that was annealed in air at 800 °C for 1.0 h.

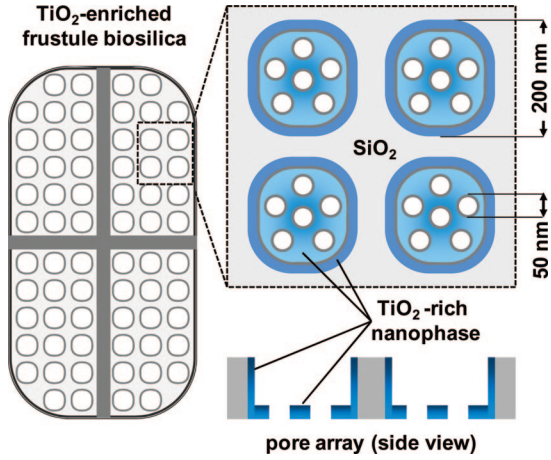

Figure 11. Conceptual illustration of TiO_2-rich nanophase in frustule biosilica (not to scale).

For the pennate diatom *Pinnularia*, we envision that following Si uptake into the diatom cell, the intracellular Si is deposited as patterned silica within the SDV of the developing valve portion of the frustule in three stages. First, parallel rib structures spanning the transapical axis of the frustule valve are symmetrically formed normal to the both sides of the center raphe. Second, silica fills in between the ribs to form the frustule pores. Finally, the thin layer of the biosilica lining the base of the 200 nm frustule pore and its associated 50 nm pores are formed.

In Stage II of cultivation, soluble Si and Ti were continuously fed to the diatom cells, but Si was always the dominant component, and the feeding rate was turned off about halfway (10 h) into the 22−25 h cell division cycle. Since the highest concentrations of titanate were observed in the fine structure associated with the final stages of silica deposition, Si pool exhaustion near the completion of frustule pore formation combined with a slower rate of soluble Ti condensation to titanate within the SDV may have been responsible for this deposition pattern.

In our previous studies with metabolic incorporation of Ge into diatom biosilica,[30−32] the high aqueous solubility of $Ge(OH)_4$ allowed all of the Ge to be added to the diatom cell suspension at the beginning of Stage II of cultivation. By this process, the germanium was uniformly dispersed into the diatom biosilica. However, due to the low aqueous solubility of $Ti(OH)_4$, simply extending this feeding approach to titanium would not work. Instead, in this study, a novel continuous feeding strategy was developed to deliver the titanium to the diatom cell. The distributed feeding of $Ti(OH)_4$ may have also contributed to the stratification of TiO_2 within the diatom biosilica.

SUMMARY

A two-stage bioreactor cultivation process was used to metabolically insert titanium into the patterned biosilica frustule of the diatom *Pinnularia* sp. by controlled feeding of soluble titanium and silicon to the silicon-starved cell culture suspension. The addition of titanium to the diatom cells had no detrimental effects on the growth of the organism and preserved the nano- and microstructure of the frustule biosilica. Co-uptake of Ti and Si was required for maximum incorporation of titanium into the frustule biosilica. Titanium was preferentially deposited as a nanophase lining the base of each frustule pore. Thermal annealing converted the biogenic titanate to nanocrystalline anatase TiO_2.

This is the first reported study of using a living organism to controllably fabricate semiconductor TiO_2 nanostructures by a bottom-up self-assembly process on a massively parallel scale. Furthermore, the cell assembles the TiO_2-rich nanostructures into clustered arrays imbedded within a photonic crystal-like structure that is characteristic of the diatom frustule. Possible device applications of these semiconductor materials could include dye-sensitized solar cells for enhanced light trapping efficiency[42] and structured photocatalysts for enhanced breakdown of toxic chemicals.[43] This study illustrates how diatom cell culture systems can be externally directed in bioprocess engineering systems to fabricate unique nano- and microstructured semiconductor materials.

MATERIALS AND METHODS

Diatom Cell Culture. The photosynthetic, pennate marine diatom *Pinnularia* sp. was obtained from the UTEX Culture Collection of Algae (UTEX# B679). Maintenance culture of this organism was previously described.[30] In this study, *Pinnularia* sp. was grown on Harrison's artificial seawater medium supplemented with f/2 nutrients[39] as modified below. The artificial seawater base medium contained 347 mM NaCl, 23.8 mM Na_2SO_4, 7.68 mM KCl, 1.97 mM $NaHCO_3$, 690 μM KBr, 354 μM H_3BO_3, 63.3 μM NaF, 45.1 mM $MgCl_2 \cdot 6H_2O$, 8.74 mM $CaCl_2 \cdot 2H_2O$, and 78.0 μM $SrCl_2 \cdot 6H_2O$. The f/2 enrichment medium components consisted of 35.9 nM $Na_2MoO_4 \cdot 2H_2O$, 0.954 nM Na_2SeO_3, 6.0 nM $NiCl_2 \cdot 6H_2O$, 165 nM $ZnSO_4 \cdot 7H_2O$, 45.3 nM $CuSO_4 \cdot 5H_2O$, 24.7 nM $CoSO_4 \cdot 7H_2O$, 2.31 μM $MnSO_4 \cdot 4H_2O$, 19.7 μM $FeCl_3 \cdot 6H_2O$, and 21.9 μM ethylenedinitrol tetraacetic acid disodium salt ($C_{10}H_{14}O_8N_2Na_2 \cdot 2H_2O$). The macronutrient medium consisted of 4.81 mM $NaNO_3$, 242 μM $NaH_2PO_4 \cdot H_2O$, and 1.00 mM $Na_2SiO_3 \cdot 9H_2O$.

Photobioreactor Cultivation. The bubble column photobioreactor for cultivation of *Pinnularia* sp. cells in liquid suspension was previously described.[30] The photobioreactor was modified to accommodate two-channel syringe pump (World Precision Instruments, Aladdin 8000) to separately deliver dissolved silicon and titanium to the cell suspension, as shown in Figure 1. Nutrient medium for cultivation of *Pinnularia* sp. in the photobioreactor was identical to the cell culture maintenance medium described above except for the dissolved silicon concentration. The CO_2 in the aeration gas served as the carbon source for phototrophic cell growth. Flask cultured diatom cells harvested 7 days after subculture were used for bioreactor inoculation.

The process conditions used in this study are summarized in Table 1. The two-stage bioreactor cultivation process described previously[30] was modified for continuous delivery of dissolved

silicon and titanium in Stage II. To prepare the Si feed solution, solid SiO_2 and NaOH were dissolved in distilled/deionized water to make 30 mM Na_2SiO_3 (sodium metasilicate) and 500 mM NaOH (pH >12). The high pH kept the silicon dissolved in the feed solution. To prepare the Ti feed solution, solid titanium hydroxide ($Ti(OH)_4$) was first made by dropwise addition of 4.0 M NaOH to aqueous titanium oxysulfate ($TiOSO_4$, 15 wt % solution, Sigma-Aldrich 495379) to pH 12, followed by precipitation at 0 °C and washing of the precipitate in deionized/distilled water. Solid $Ti(OH)_4$ and concentrated HCl were then dissolved in HPLC-grade water to final concentrations of 5.0 mM Ti and 500 mM HCl (pH <1). The low pH kept the titanium soluble in aqueous solution. To prepare a Ti feed solution of a desired concentration, the 5.0 mM Ti stock solution was diluted in distilled/deionized water, and then concentrated HCl was added to bring the HCl concentration back up to 500 mM. The volumetric flow rate of the Si and Ti feed solutions to the photobioreactor culture suspension was each fixed at 5.0 mL h^{-1} for a total of 10 h, beginning 2 h into the photoperiod. When the Si and Ti feed solutions were added to the culture suspension at the same volumetric flow rate, the NaOH in the Si feed solution and HCl in the Ti feed solution were neutralized, resulting in no pH change to the culture medium.

Cell number density and dry cell weight (DW) measurements of the diatom cell suspension were previously described.[30] In Stage I of cultivation, the cell suspension was sampled every 12 h until 120 h, whereas in Stage II, the cell suspension was sampled every 3 h during the initial 12 h, and then every 12 h until 72 h. A cell culture volume of 540 mL was removed at 0, 12, 24, 48, and 72 h of Stage II to determine the silicon and titanium content in the dry cell biomass and frustule biosilica. The liquid medium was separated from the diatom cells by centrifugation at 2500*g* for 20 min. The concentrations of silicon and titanium in the liquid medium were determined by inductively coupled plasma emission spectroscopy (ICP-ES) analysis on a Varian Liberty 150 ICP emission spectrometer. Analysis wavelengths were 251.611 (Si) and 334.941 nm (Ti). Limits of detection were 0.07 and 0.004 mg/L for Si and Ti, respectively. The silicon and titanium content in the dry cell mass was also determined by ICP-ES following NaOH fusion of the solid as previously described.[30] Statistical estimation of specific growth rate (μ, h^{-1}) and cell number yield coefficient ($Y_{Xn/Si}$, cells/mmol Si consumed) were previously described.[30]

Isolation and Bulk Metal Analysis of Frustule Biosilica. Intact biosilica frustules of *Pinnularia* sp. cells were isolated by treatment with sodium dodecyl sulfate (SDS, JT Baker L050-07) and ethylene diamine tetraacetic acid (EDTA), as originally described by Schmid and Schulz,[40] with modifications detailed below. Treatment of diatom cells with the detergent SDS separated organic cell matter from the frustule biosilica but did not remove the girdle band proteins, and so the upper and lower theca of the frustule remained attached. The EDTA removed calcium and other divalent salts from the seawater medium that adsorbed onto the frustule surface. Duplicate 250 mL aliquots of culture suspension were centrifuged at 2500*g* for 20 min. The pellet was resuspended in 40 mL of distilled/deionized water, centrifuged, and washed again two more times. The washed diatom cell pellet was resuspended in 40 mL of 50 g/L SDS in 100 mM EDTA, vortexed for 1 min, and then allowed to react for 20 min at room temperature without mixing. The liquid in the suspension turned green. The SDS/EDTA treatment was repeated two more times. The treated cell mass was washed three times in distilled/deionized water to remove the SDS/EDTA and residual intracellular metal oxides, and then three times in methanol to dissolve the residual organic matter (40 mL, 2500*g* for 20 min). The final isolated frustules were resuspended in 5 mL of MeOH and stored at −20 °C. The silicon and titanium content in the isolated frustule solid was determined by ICP-ES as described above. The titanium content was expressed as g of Ti/100 g of SiO_2, assuming that the Si in the frustule was in the form of SiO_2. Isolation of diatom biosilica by aqueous hydrogen peroxide treatment of diatom cells was previously described.[30]

Thermal Annealing and X-ray Diffraction Analysis. A 10 mg aliquot of frustule biosilica isolated by SDS/EDTA treatment was thermally annealed in air for 1.0 h within a preheated furnace at temperatures of 720, 800, and 950 °C. Powder X-ray diffraction (XRD) measurements on the as-deposited and thermally annealed frustule biosilica were performed on a Bruker Instruments D8 Discover diffractometer using a Cu Kα radiation source. Full scans (2θ 20−80°) were performed at step size of 0.05° and scan rate of 5.0 2θ/min, whereas limited scans near the highest TiO_2 peaks of interest (2θ 23−28°) were performed at a scan rate of 0.5 2θ/min. Peaks were compared to standards for anatase TiO_2 (JCPDS database #86-1156) and rutile TiO_2 (JCPDS database #86-0148). The size of each TiO_2 nanocrystal type was estimated from the angle and half-width of its strongest peak using the well-known Scherrer equation.[41]

Electron Microscopy. Electron microscopy analyses on *Pinnularia* sp. frustules isolated by SDS/EDTA treatment were performed on a FEI Tecnai F20 high resolution (200 keV) transmission electron microscope (TEM) equipped with an embedded scanning transmission electron microscope (STEM) and an X-ray energy dispersive analysis (EDS) probe, as previously described.[30] SEM images were obtained on an FEI Sirion field emission SEM at an accelerating voltage of 5 keV. All STEM-EDS data were collected at an accelerating voltage of 200 keV. The K_α energy peaks of interest were 0.52 (O), 1.74 (Si), and 4.51 keV (Ti). The beam resolution was 0.24 nm for spot analysis and 0.18 nm for line analysis. The local TiO_2 content in frustule biosilica along the STEM-EDS elemental line scan was estimated by

$$Y_{TiO_2} = \frac{I_{Ti,c} k_{Ti} M_{TiO_2} / M_{Ti}}{I_{Ti,c} k_{Ti} M_{TiO_2} / M_{Ti} + I_{Si} k_{Si} M_{SiO_2} / M_{Si}} \quad (1)$$

and

$$I_{Ti,c} = I_{Ti} - (m_{Ti} \cdot I_{Si} + I_{Ti,o}) \quad (2)$$

where $I_{Ti,c}$ is the Ti detector count corrected for Ti background signal in silica, I_{Si} is the Si detector count, k_{Ti} is the calibration *k* factor for Ti (1.299 mass counts/detector counts), k_{Si} is the calibration *k* factor for Si (1.000 mass counts/detector counts), M_{Si} and M_{SiO_2} are the molecular weights of Si and SiO_2, and M_{Ti} and M_{TiO_2} are the molecular weights of Ti and TiO_2. The corrected Ti detector count was estimated by eq 2, where I_{Ti} is the gross Ti count, m_{Ti} is the ratio of Ti background counts to Si counts, and $I_{Ti,o}$ is the Ti background count in the absence of Si. Values for m_{Ti} (4.0 Ti counts/1000 Si counts) and $I_{Ti,o}$ (3 counts) were determined by linear regression of Si and Ti counts pooled from EDS line scans over frustules obtained by the control cultivation experiment where no Ti was added to the diatom cell suspension. Energy peaks associated with the holey carbon copper (Cu) TEM grid also appeared in the EDS spot scan spectra (L_3 at 0.93 keV, K_α at 8.05 keV, K_β at 8.90 keV).

Acknowledgment. This research was supported by the National Science Foundation (NSF) under Nanoscale Interdisciplinary Research Team (NIRT) award number BES-0400648.

REFERENCES AND NOTES

1. Chen, X.; Mao, S. S. Titanium Oxide Nanomaterials: Synthesis, Properties, Modifications, and Applications. *Chem. Rev.* **2007**, *107*, 2891–2959.
2. Aprile, C.; Corma, A.; Garcia, H. Enhancement of the Photocatalytic Activity of TiO_2 through Spatial Structuring and Particle Size Control: From Subnanometric to Submillimetric Length Scale. *Phys. Chem. Chem. Phys.* **2008**, *10*, 769–783.
3. Sarikaya, M.; Tamerler, C.; Jen, A. K. Y.; Schulten, K.; Baneyx, F. Molecular Biomimetics: Nanotechnology through Biology. *Nat. Mater.* **2003**, *2*, 577–585.
4. Parker, A. R.; Townley, H. E. Biomimetics of Photonic Nanostructures. *Nat. Nanotechnol.* **2007**, *2*, 347–353.
5. Cole, K. E.; Valentine, A. M. Titanium Biomaterials: Titania Needles in the Test of the Foraminiferan *Bathysiphon argenteus*. *Dalton Trans.* **2006**, 430–432.

6. Sumper, M.; Brunner, E. Learning from Diatoms: Nature's Tools for the Production of Nanostructured Silica. *Adv. Funct. Mater.* **2006**, *16*, 17–26.
7. Yamanaka, S; Yano, R.; Hisanao, U.; Hayashida, N.; Ohguchi, M.; Takeda, H.; Yoshino, K. Optical Properties of Diatom Silica Frustule with Special Reference to Blue Light. *J. Appl. Phys.* **2008**, *103*, 074701.
8. Kröger, N.; Dickerson, M. B.; Ahmad, G.; Cai, Y.; Haluska, M. S.; Sandhage, K. H.; Poulsen, N.; Sheppard, V. C. Bioenabled Synthesis of Rutile (TiO_2) at Ambient Temperature and Neutral pH. *Angew. Chem., Int. Ed.* **2006**, *45*, 7239–7243.
9. Cole, K. E.; Ortiz, A. N.; Schoonen, M. A.; Valentine, A. M. Peptide and Long-Chain Polyamine Induced Synthesis of Micro- and Nanostructured Titanium Phosphate and Protein Encapsulation. *Chem. Mater.* **2006**, *18*, 4592–4599.
10. Sewell, S. L.; Wright, D. W. Biomimetic Synthesis of Titanium Dioxide Utilizing the R5 Peptide Derived from *Cylindrotheca fusiformis*. *Chem. Mater.* **2006**, *18*, 3108–3113.
11. Dickerson, M. B.; Jones, S. E.; Cai, Y.; Ahmad, G; Naik, R. R.; Kröger, N.; Sandhage, K. H. Identification and Design of Peptides for the Rapid, High-Yield Formation of Nanoparticulate TiO_2 from Aqueous Solutions at Room Temperature. *Chem. Mater.* **2008**, *20*, 1578–1584.
12. Sumerel, J. L.; Yang, W.; Kisailus, D.; Weaver, J. C.; Choi, J. H.; Morse, D. E. Biocatalytically Templated Synthesis of Titanium Dioxide. *Chem. Mater.* **2003**, *15*, 4804–4809.
13. Tahir, M. N.; Théato, P; Müller, W. E. G.; Schröder, H. C.; Borejko, A.; Faiss, S.; Janshoff, A.; Huth, J.; Tremel, W. Formation of Layered Titania and Zirconia Catalyzed by Surface Bound Silicatein. *Chem. Commun.* **2005**, 5533–5535.
14. Brutchey, R. L.; Yoo, E. S.; Morse, D. E. Biocatalytic Synthesis of a Nanostructured and Crystalline Biomimetic Perovskite-like Barium Oxofluorotitanate at Low Temperature. *J. Am. Chem. Soc.* **2006**, *128*, 10288–10294.
15. Cole, K. E.; Valentine, A. M. Spermidine and Spermine Catalyze the Formation of Nanostructured Titanium Oxide. *Biomacromolecules* **2007**, *8*, 1641–1647.
16. Luckarift, H. R.; Dickerson, M. B.; Sandhage, K. H.; Spain, J. C. Rapid, Room Temperature Synthesis of Antibacterial Bionanocomposites of Lysozyme with Amorphous Silica or Titania. *Small* **2006**, *2*, 640–643.
17. Bansal, V.; Rautaray, D.; Bharde, A.; Ahire, K.; Sanyal, A.; Ahmad, A.; Sastry, M. Fungus-Mediated Biosynthesis of Silica and Titania Particles. *J. Mater. Chem.* **2005**, *15*, 2583–2589.
18. Curnow, P.; Bessette, P. H.; Kisailus, D.; Murr, M. M.; Daugherty, P. S.; Morse, D. E. Enzymatic Synthesis of Layered Titanium Phosphates at Low Temperature and Neutral pH by Cell-Surface Display of Silicatein-α. *J. Am. Chem. Soc.* **2005**, *127*, 15749–15755.
19. Unocic, R. R.; Zalar, F. M.; Sarosi, P. M.; Cai, Y.; Sandhage, K. Anatase Assemblies from Algae: Coupling Biological Self Assembly of 3-D Nanoparticle Structures with Synthetic Reaction Chemistry. *Chem. Commun.* **2004**, 796–797.
20. Dudley, S.; Kalem, T.; Akinc, M. Conversion of SiO_2 Diatom Frustules to $BaTiO_3$ and $SrTiO_3$. *J. Am. Ceram. Soc.* **2006**, *89*, 2434–2439.
21. Losic, D.; Triani, G.; Evans, P. J.; Atanacio, A.; Mitchell, J. G.; Voelcker, N. H. Controlled Pore Structure Modification of Diatoms by Atomic Layer Deposition of TiO_2. *J. Mater. Chem.* **2006**, *16*, 4029–4034.
22. Jia, Y.; Xiong, G.; Yang, W. Layer-by-Layer Assembly of TiO_2 Colloids onto Diatomite to Build Hierarchical Porous Materials. *J. Colloid Interface Sci.* **2008**, *323*, 326–331.
23. Riley, J. P.; Roth, I. The Distribution of Trace Elements in Some Species of Phytoplankton Grown in Culture. *J. Mar. Biol. Assoc. U.K.* **1971**, *51*, 63–72.
24. Martin, J. H.; Knauer, G. A. The Elemental Composition of Plankton. *Geochim. Cosmochim. Acta* **1973**, *37*, 1639–1653.
25. Martin-Jézéquel, V; Hildebrand, M.; Brzeziniski, M. A. Silicon Metabolism in Diatoms: Implications for Growth. *J. Phycol.* **2000**, *36*, 821–840.
26. Baes, C. F.; Mesmer, R. E. *The Hydrolysis of Cations*; Wiley-Interscience: New York, 1976.
27. Sugimoto, T.; Zhou, X.; Muramatsu, A. Synthesis of Uniform Anatase TiO_2 Nanoparticles by Gel−Sol Method. 1. Solution Chemistry of $Ti(OH)_n^{(4-1)+}$ Complexes. *J. Colloid Interface Sci.* **2002**, *252*, 339–346.
28. Goldstein, J. I.; Newbury, D. E.; Joy, D. C.; Lyman, C.; Echlin, P.; Lifshin, E.; Sawyer, L.; Michael, J. *Scanning Electron Microscopy and X-ray Microanalysis*, 3rd ed.; Kluwer Academic−Plenum: New York, 2003.
29. Newbury, D. E. Quantitative Electron Probe Microanalysis of Rough Targets: Testing the Peak-to-Local Background Method. *Scanning* **2004**, *26*, 103–114.
30. Jeffryes, C.; Gutu, T.; Jiao, J.; Rorrer, G. L. Two-Stage Photobioreactor Process for the Metabolic Insertion of Nanostructured Germanium into the Silica Microstructure of the Diatom *Pinnularia* sp. *Mater. Sci. Eng. C* **2008**, *28*, 107–118.
31. Jeffryes, C.; Solanki, R.; Rangineni, Y.; Wang, W.; Chang, C.-H.; Rorrer, G. L. Electroluminescence and Photoluminescence from Nanostructured Diatom Frustules Containing Metabolically Inserted Germanium. *Adv. Mater.* **2008**, *20*, 2633–2637.
32. Qin, T.; Gutu, T.; Jiao, J.; Chang, C.-H.; Rorrer, G. L. Biological Fabrication of Photoluminescent Nanocomb Structures by Metabolic Incorporation of Germanium into the Biosilica of the Diatom *Nitzschia frustulum*. *ACS Nano* **2008**, *2*, 1296–1304.
33. Round, F. E.; Crawford, R. M.; Mann, D. G. *The Diatoms*; Cambridge University Press: Cambridge, 1990.
34. van den Hoek, C.; Mann, D. G.; Jahns, H. M. *Algae: An Introduction to Phycology*; Cambridge University Press: Cambridge, 1995.
35. Pickett-Heaps, J. D.; Tippit, D. H.; Andreozzi, J. A. Cell Division in the Pennate Diatom *Pinnularia*. IV−Valve Morphogenesis. *Biol. Cellulaire* **1979**, *35*, 199–203.
36. Sumper, M. A Phase Separation Model for the Nanopatterning of Diatom Biosilica. *Science* **2002**, *295*, 2430–2433.
37. Lenoci, L.; Camp, P. J. Diatom Structures Template by Phase-Separated Fluids. *Langmuir* **2008**, *24*, 217–223.
38. Hildebrand, M.; York, E.; Kelz, J. I.; Davis, A. K.; Frigeri, L. G. Nanoscale Control of Silica Morphology and Three-Dimensional Structure during Diatom Cell Wall Formation. *J. Mater. Res.* **2006**, *21*, 2689–2698.
39. Harrison, P. J.; Waters, R. E.; Taylor, F. J. R. A Broad Spectrum Artificial Seawater Medium for Coastal and Open Ocean Phytoplankton. *J. Phycol.* **1980**, *16*, 28–25.
40. Schmid, A.; Schulz, D. Wall Morphogenesis in Diatoms: Deposition of Silica by Cytoplasmic Vesicles. *Protoplasma* **1979**, *100*, 289–301.
41. Scherrer, P. Bestimmung de Grösse und der inneren Struktur von Kolloidteilchen mittels Röntgenstrahlen. *Göttinger Nachrichten* **1918**, *2*, 98–100.
42. Mihi, A.; Calvo, M. E.; Anta, J. A.; Miguez, H. Spectral Response of Opal-Based Dye-Sensitized Solar Cells. *J. Phys. Chem. C* **2008**, *112*, 13–17.
43. Carbonell, E.; Ramiro-Manzano, F.; Rodriguez, I.; Corma, A.; Meseguer, F.; Garcia, H. Enhancement of TiO_2 Photocatalytic Activity by Structuring the Photocatalyst Film as a Photonic Sponge. *Photochem. Photobiol. Sci.* **2008**, *7*, 931–935.